Optimization of Crop Canopy Sensor Placement for Measuring Nitrogen Status in Corn

Darrin F. Roberts,* Viacheslav I. Adamchuk, John F. Shanahan, Richard B. Ferguson, and James S. Schepers

ABSTRACT

Active canopy sensors can be used to assess corn (*Zea mays* L.) N status and direct spatially-variable in-season N application. The goal of this study was to determine optimal sensor spacing for controlling whole- and/or split-boom N application scenarios for a hypothetical 24-row applicator. Sensor readings were collected from 24 consecutive rows at eight cornfields during vegetative growth in 2007 and 2008, and readings were converted to chlorophyll index (CI) values. A base map of measured CI values was created using square pixels equal to row spacing for each site (0.91 or 0.76 m in size). Sensor placement and boom section scenarios were evaluated using MSE (mean squared error) of calculated CI maps vs. the base CI map. Scenarios ranged from one sensor, one variable-rate to 24 sensors, 24 variable-rates for the hypothetical 24-row applicator. The greatest reduction in MSE from the one variable-rate scenario was obtained with 2 to 3 sensors estimating average CI for the entire boom width, unless each row was individually sensed. In every field, more accurate prediction of CI was obtained by averaging sensor readings across the entire 24 rows rather than predicting CI for more than two consecutive rows using only one sensor in each section. Because of the nature of spatial variability in CI, some fields may benefit from an increased number of sensors and/or boom sections equipped with 2 to 3 sensors each.

Worldwide N fertilizer application for cereal crops has reached ~84 million megagrams per year (FAO, 2008). Under current N management practices, much of this applied N is not fully used, as fertilizer recovery has been estimated as low as 33 to 37% (Raun and Johnson, 1999; Cassman et al., 2002). This unused N is at risk of being lost to the environment either as gaseous losses or through runoff and leaching, resulting in contaminated air and water resources, and represents a substantial economic loss for producers.

Two causes of low nitrogen use efficiency (NUE) are poor synchrony between soil N supply and crop demand and uniform application rates of fertilizer N to spatially-variable landscapes (Shanahan et al., 2008). Nitrogen applied in the fall or before a crop is established in the spring fails to account for crop N demand and spatial variability of N needs, and thereby leads to reduced NUE. Conversely, Varvel et al. (1997) and later Varvel et al. (2007) found that "spoon-feeding" N fertilizer based on leaf greenness measurements using a SPAD chlorophyll meter could be used to reduce N applications while maintaining near-optimum yields. However, extending this tool and concept to whole-field management is problematic since it is extremely difficult to collect sufficient data using a hand-held device to manage large fields (Schepers et al., 1995). Remote sensing offers a practical means to assess spatial variability in fields across large areas (Scharf et al., 2002). In recent years, active crop canopy sensors have been studied as a possible remote sensing tool to accurately assess in-season plant N status and direct spatially-variable N applications (Solari et al., 2008; Raun et al., 2002). Active canopy sensors generate modulated light in the visible (400–700 nm) and near-infrared (NIR) (700–1000 nm) regions of the electromagnetic spectrum. Past research in wheat (*Triticum aestivum* L.) determined an appropriate algorithm to convert light reflectance measurements at two preselected wavelengths into N application rates (Raun et al., 2005).

Solie et al. (1996) evaluated the optimal spatial scale for sensing and applying N in wheat, and found that spatial scales greater than ~2 m^2 would likely not optimize fertilizer N inputs and had potential for inaccurate N application. For Bermudagrass [*Cynodon dactylon* (L.) Pers.], Solie et al. (1999) concluded 1 m^2 or less to be the optimal spatial scale for which variable-rate equipment should be able to sense and apply fertilizer. Raun et al. (2002) was able to improve winter wheat NUE > 15% by varying the N rate at the 1-m^2 scale. More recently, Pena-Yewtukhiw et al. (2008) found that the spatial scale could be increased to 5.1 m^2 without significantly affecting the measured spatial structure of a canopy vegetative index.

While a considerable amount of research has been conducted to establish the optimal spatial scale for sensing and N application to wheat, little work has been performed to establish the appropriate spatial scale for corn. Because of likely high costs associated with active sensors and control equipment to vary N rates for individual rows, there is need to identify an optimal strategy for sensor placement on application booms. Therefore,

D.F. Roberts and R.B. Ferguson, Dep. of Agronomy & Horticulture, Univ. of Nebraska, Lincoln, NE 68583; V.I. Adamchuk, Dep. of Biological Systems Engineering, Univ. of Nebraska, Lincoln, NE 68583; J.F. Shanahan, USDA-ARS, Agroecosystem Mgmt. Res. Unit, Lincoln, NE 68583; J.S. Schepers, retired, formerly USDA-ARS, Agroecosystem Mgmt. Res. Unit, Lincoln, NE 68583. Received 30 Aug. 2008. *Corresponding author (droberts2@unl.edu).

Published in Agron. J. 101:140–149 (2009).
doi:10.2134/agronj2008.0072x

Abbreviations: CI, chlorophyll index; MSE, mean squared error; NUE, nitrogen use efficiency; NIR, near-infrared.

the objective of this study was to determine optimal sensor spacing for controlling whole- and/or split-boom N application scenarios for a hypothetical 24-row applicator.

MATERIALS AND METHODS

Research Fields

This research was conducted in eight sprinkler-irrigated producer fields located in central Nebraska during the 2007 and 2008 growing seasons (Table 1). Hybrid selection and all field operations were performed by the producers. Fields 1, 2, 3, 4, and 5 were planted with rows oriented in the east–west direction, while rows for Fields 6, 7, and 8 were planted in the north–south direction. Rows were 300 to 400 m in length for all fields except Field 5 (650 m) and Field 6 (750 m).

In Fields 2 and 4, the producers applied all N fertilizer at or shortly after planting (~170 kg ha^{-1}). Study areas in Fields 1 and 3 received ~20 kg N ha^{-1} from starter fertilizer applied at planting, 45 kg ha^{-1} and 123 kg ha^{-1} uniform N application, respectively, applied as urea-ammonium-nitrate (UAN) solution at the V6 growth stage followed by a supplemental in-season N application (part of a different study) after in-season sensor measurements were collected. Fields 5 and 6 received 90 kg N ha^{-1} and 45 kg N ha^{-1}, respectively, applied as UAN solution shortly after emergence. Supplemental fertilizer was applied to Fields 5 and 6 after the time of sensor data acquisition. Fields 7 and 8 received all N fertilizer (~170 kg ha^{-1}) as sidedress (~V8 growth stage) UAN solution. The various N application rates and plant growth stages (Table 1) provided a broad range of plant height, biomass accumulation, and chlorophyll content during the time in-season N application would likely occur.

Active Canopy Reflectance Sensors

The active canopy reflectance sensor used for this study was the ACS-210 Crop Circle (Holland Scientific, Inc., Lincoln, NE). This sensor generates modulated light in the visible and NIR regions of the electromagnetic spectrum and measures canopy reflectance with visible (590 ± 5.5 nm, VIS_{590}) and NIR detectors (880 ± 10 nm, NIR_{880}). The VIS_{590} band was selected in constructing the Crop Circle sensor in lieu of the green band (560 nm) studied by Gitelson et al. (2003 and 2005) because the electro-optical characteristics for various combinations of commercially available photodiodes and filters provided better measurement performance characteristics in the 590-nm band than in the 560-nm band (Solari et al., 2008). However, this is not problematic because the sensitivity of reflectance to chlorophyll content remains high and relatively constant in a wide spectral range from 530 through 600 nm (Gitelson et al., 1996). Sensor reflectance in the VIS_{590} and NIR_{880} was used to calculate CI_{590} values according to Gitelson et al. (2003) and Gitelson et al. (2005) using the following equation:

$$CI_{590} = \frac{NIR_{880}}{VIS_{590}} - 1 \quad [1]$$

Sensor-based CI_{590} values were used in lieu of the more traditional NDVI because CI_{590} was found to be more sensitive in assessing canopy N status than NDVI (Solari et al., 2008).

Acquisition of Canopy Reflectance Data

To acquire active sensor readings, four Crop Circle sensors were mounted on an adjustable-height boom (on the rear in 2007 and front in 2008) of a high-clearance vehicle and maintained at a distance of approximately 0.8 to 1.5 m above the crop canopy. The sensors were positioned directly over each row in the nadir view, producing a footprint of approximately 0.1 by 0.5 m, with the long dimension of this footprint oriented perpendicular to the row direction. This sensor position was determined to be optimal for assessing canopy N status by Solari (2006). Before field operation, each of four sensors was calibrated by the manufacturer using a proprietary universal 20% reflectance panel with the sensor placed in the nadir position above the panel (personal communication, Holland Scientific, Inc., 2008). The output from each sensor included pseudo-reflectance values for the two parts of the spectrum needed for CI calculation.

Canopy sensor data were collected from 24 consecutive rows within each field. Six consecutive passes were conducted to collect data from each study area within every field. This study width was selected because it was a multiple of producer equipment (8 and 12 rows) for all fields in the dataset. This width provided a minimum distance to assess spatial structure of CI perpendicular to the direction of travel and any potential management induced effects on CI, although greater study widths could have been selected.

A Garmin 18 (Garmin International, Inc., Olathe, KS) Global Positioning System (GPS) receiver with an update rate

Table 1. Producer practices, corn growth stage at the time of in-season data collection, soil series, and soil classification for Fields 1–8.

Field ID	Year	Row spacing	Producer equipment width	Growth stage	Soil series	Soil classification
		m	rows			
1	2007	0.91	8	V11	Hord silt loam	fine-silty, mixed, mesic Pachic Haplustoll, 0–1% slope
2	2007	0.91	8	V9	Gibbon silt loam	fine-silty, mixed, mesic Fluvaquentic Endoaquoll, 0–2% slope
3	2007	0.91	8	V14	Hord silt loam	fine-silty, mixed, mesic Pachic Haplustoll, 0–1% slope
4	2007	0.91	12	V17	Hord silt loam	fine-silty, mixed, mesic Pachic Haplustoll, 0–1% slope
5	2008	0.76	12	V10	Valentine fine sand	mixed, mesic Typic Ustipsamment, 9–24% slope
					Thurman loamy fine sand	sandy, mixed, mesic Udorthentic Haplustoll, 2–6% slope
6	2008	0.76	24	V13	Hastings silt loam	fine, smectitic, mesic Udic Arguistoll, 0–1% slope
					Hastings silty clay loam	fine, smectitic, mesic Udic Arguistoll, 3–7% slope, eroded
					Hastings silty clay loam	fine, smectitic, mesic Udic Arguistoll, 7–11% slope, eroded
7	2008	0.91	8	V15	Detroit silt loam	fine, smectitic, mesic Pachic Argiustoll, 0–1% slope
8	2008	0.91	8	V15	Detroit silt loam	fine, smectitic, mesic Pachic Argiustoll, 0–1% slope

Table 2. Sensor placement scenarios considered for the 24 rows from each of the 8 fields. Row numbers selected in each scenario were assumed to represent a logical placement of sensors for a 24 row applicator, although other rows could have been selected. In rows without a sensor (Scenarios 2–8), chlorophyll index estimates were either obtained from the nearest row with a sensor or as an average from all 24 rows. Row numbers used in data analysis are indicated for each scenario.

Scenario	Row number for sensor whose measurements are used as predictor (substitute sensor) for the given row																							
1. Every row	1	2	3	4	5	6	7	8	9	10	11	12	13	14	15	16	17	18	19	20	21	22	23	24
2. Every other row	1	1	3	3	5	5	7	7	9	9	11	11	13	13	15	15	17	17	19	19	21	21	23	23
3. Every 3 rows	2	2	2	5	5	5	8	8	8	11	11	11	14	14	14	17	17	17	20	20	20	23	23	23
4. Every 4 rows	2	2	2	2	6	6	6	6	10	10	10	10	14	14	14	14	18	18	18	18	22	22	22	22
5. Every 6 rows	4	4	4	4	4	4	9	9	9	9	9	9	16	16	16	16	16	16	21	21	21	21	21	21
6. Every 8 rows	4	4	4	4	4	4	4	4	13	13	13	13	13	13	13	13	20	20	20	20	20	20	20	20
7. Every 12 rows	6	6	6	6	6	6	6	6	6	6	6	6	19	19	19	19	19	19	19	19	19	19	19	19
8. Every 24 rows	12	12	12	12	12	12	12	12	12	12	12	12	12	12	12	12	12	12	12	12	12	12	12	12

of 5 Hz was mounted in the center on top of the vehicle cab and offset 2.4 m from the sensor boom. Canopy reflectance measurements were collected at 10 Hz while the vehicle traveled at a ground speed ~8 km h^{-1}, resulting in raw data points ~0.22 m apart. Linear interpolation was applied to assign unique geographic coordinates to each recorded measurement. Geographic coordinates were adjusted to account for the sensor boom offset relative to GPS antenna position. A base map for each study area was created by averaging between three and five sensor measurements placed within each square pixel equal to row spacing (0.91 × 0.91 m for Fields 1, 2, 3, 4, 7, and 8; 0.76 × 0.76 m for Fields 5 and 6). It was assumed that this base map represented the finest spatial resolution for sensor measurements and provided the greatest spatial detail for prescribing N applications. Every map obtained using a reduced sensor number was evaluated against this "base" map.

Statistical Analysis of Canopy Reflectance Data

Lateral (across the boom) and direction-of-travel semivariograms were calculated to assess the spatial structure of each study area. Lateral semivariance (γ) was calculated using the following equation:

$$\gamma(r)=\frac{1}{2L(M-r)}\sum_{j=1}^{L}\sum_{i=1}^{M-r}\left[\mathrm{CI}_{ij}-\mathrm{CI}_{(1+r)j}\right]^2 \qquad [2]$$

where r is a separation distance (number of rows between sensor measurements) ranging from 1 to 23, $M = 24$ is the total number of rows, L is the number of pixels in the direction of travel (ranging from 1 to 100 for the calculation), and CI_{ij} is the chlorophyll index corresponding to the ith row and jth position along that row. Direction-of-travel semivariance was calculated using the same equation after interchanging L and M.

For the empirical study, eight sensor placement scenarios were considered for this study (Table 2). Sensor placement ranged from dense spacing across the boom (over every row) to one sensor for the entire study area (24 rows). Row numbers selected in each scenario were assumed to represent a logical placement of sensors for a 24-row applicator, although other rows could have been selected. In rows that did not have sensors, CI estimates were either obtained from the nearest row with a sensor (split-boom scenarios), or as an average from all 24 rows (whole-boom scenarios). The MSE was calculated as the average of squared differences between actual (base map) and calculated (predicted map) CI values for each pixel.

Although combinations of rows with sensors shown in Table 2 provide a valid set of empirical scenarios, other combinations could be chosen as well. Assuming that sensor locations can be randomly assigned to any row within a section of the boom, the following equation was derived to quantify MSE (see Adamchuk et al., 2004):

$$\mathrm{MSE}=\sigma_m^2\left(\frac{n-1}{m}+\frac{m-n}{m}\times\frac{1+n}{n}\right) \qquad [3]$$

where σ_m^2 is the variance of CI sensor measurements per m consecutive rows, n is the number of sensors per each boom section, and m is the number of rows per each boom section. Assuming that the boom can be split into z number of sections with equal number of rows, the total number of rows $M = m \times z$, and the total number of sensors $N = n \times z$ (n can range from 1 to m). Because 24 rows were used to create the base map ($M = 24$), feasible scenarios included $z = 1$, 2, 3, 4, 6, 8, 12, and 24, which means $m = 24$, 12, 8, 6, 4, 3, 2, and 1, respectively.

In the case where average CI is applied to the entire 24-row boom ($z = 1$), Eq. [3] can be rewritten as:

$$\mathrm{MSE}=\sigma_M^2\left(\frac{1+n}{n}\times\frac{M-n}{M}+\frac{n-1}{M}\right) \qquad [4]$$

where σ_M^2 is the variance of CI sensor measurements for the entire M-row boom, $M = m = 24$, and $n = N$. In this equation, the $(1 + n)/n$ factor provides the penalty for a limited number of sensors used to predict the average. This penalty is applied only to those rows that do not have sensors ($M - n$). Errors corresponding to the rows with sensors (n) are assigned values equal to the average squared difference between actual sensor measurements and their mean.

Similarly, one sensor per split-boom section scenarios ($z = N$ and $n = 1$) yielded the following derivative of Eq. [4]:

$$\mathrm{MSE}=2\sigma_m^2\left(\frac{M-z}{M}\right) \qquad [5]$$

In this case, we assumed that rows with a sensor did not have any measurement error, while rows without a sensor ($M - z$) had errors equal to the doubled variance of sensor measurements in a corresponding section of the boom (m rows). Both empirical and analytical estimates of MSE were used to identify the most suitable distribution of sensors along a 24-row boom.

In addition, MSE values were compared with the CI variance along rows. To gain the benefit of variable-rate N management, these MSE estimates should be much lower than MSE estimates obtained under the assumption of an average CI for

the entire study area as well as for individual rows. Since our preliminary considerations suggested an eight-row symmetrical CI systematic pattern in four fields, an additional analysis was performed to see if predictability of row-to-row variability could reduce MSE.

RESULTS AND DISCUSSION

Spatial Structure

Descriptive statistics calculated for sensor determined CI values (Fig. 1) illustrates that average CI differed greatly across the eight study fields, with the lowest mean CI occurring at Fields 5 and 6 and highest at Fields 7 and 8. Likewise, the range in CI values varied across fields, with the greatest range in CI occurring at Fields 5 and 6, and lesser variation occurring at the other fields. Thus, the eight fields provided a considerable range in variation of measured CI values for addressing our study objectives.

Semivariance analysis of lateral (along the boom) CI values (Fig. 2A), shows there was no substantial relationship between row spacing and measured semivariance of CI for Fields 1–4. Semivariance fluctuated between 0.15 and 0.4 starting at one-row (0.91 m) separation distance. This means that, in general, two neighbor rows have the same expected differences as those 23 rows apart. Of the 2007 fields, only Field 2 indicated some (<0.005 m^{-1}) increase of semivariance with separation distance. However, in 2008 Fields 5, 6, and 8 all exhibited varying degrees of spatial dependency, with semivariance increasing with separation distance (Fig. 2B). Field 5 showed an increase in semivariance up to 3 m; thereafter, semivariance generally cycled around 0.7 to 0.8. Lateral semivariance measured in Field 6 increased steadily from 0.28 at 0.76-m separation to 0.46 at 5.3-m separation, and continued to increase gradually up to the maximum lateral separation distance. Lateral semivariance increased slightly with separation distance in Field 8 (0.008 m^{-1}), while semivariance in Field 7 remained constant at 0.11. It was noted that Fields 1, 2, 3, and 5 had four-row systematic patterns with different levels of magnitude. These patterns could possibly be attributed to management-induced variability including soil P deficiency, nonuniform starter fertilizer placement, soil compaction due to controlled traffic, and/or distribution pattern of crop residue from the previous crop. Since each sensor was calibrated using the same procedure and a systematic pattern in Fields 4, 6, 7, and 8 was not measured, it was concluded that these systematic patterns were not sensor-induced.

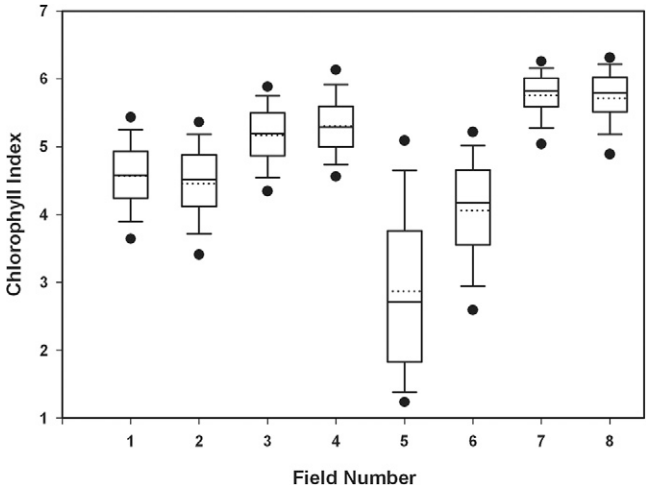

Fig. 1. Box-and-whiskers diagram of Chlorophyll Index (CI) base maps for Fields 1–8. The lower and upper limits of each box signify the 25th and 75th percentiles of CI, the lower and upper whiskers represent the 10th and 90th percentiles of CI, the large dots indicate the 5th and 95th percentiles of CI, the horizontal line in the center of each box represents the median, and the dotted line represents the mean of CI values.

Direction-of-travel semivariograms (Fig. 2C) indicated that Field 2 had significant spatial structure where semivariance

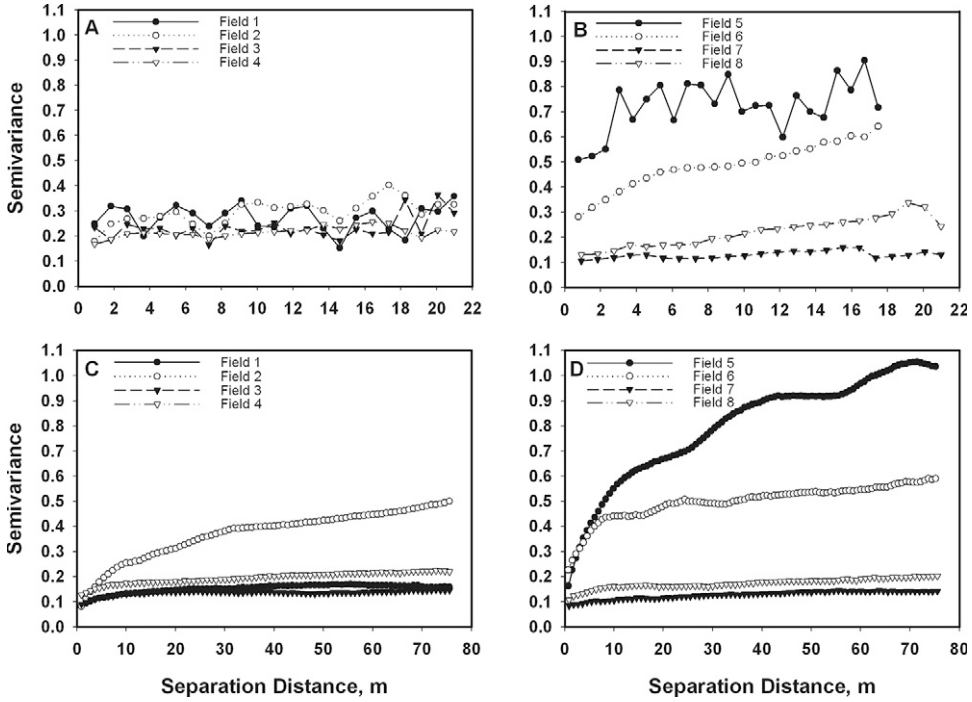

Fig. 2. Lateral (A, B) and direction-of-travel (C, D) semivariograms of chlorophyll index for Fields 1 through 8.

increased from 0.08 at 1 m to 0.39 at 32 m, and further to 0.5 at 75 m separation distance. The spatial structure for Fields 1, 3, 4, 7, and 8 was much weaker (less than lateral semivariance estimates) with semivariance reaching only 0.17, 0.14, 0.22, 0.14, and 0.20 (<80 m separation distance), respectively (Fig. 2C and 2D). The consistent change of CI along rows measured in Field 2, as compared with Fields 1, 3, and 4, was potentially related to variability of crop stand due to high soil water content at the time of planting impacting some areas of the field. In addition, sensing of Field 2 occurred at an earlier growth stage than Fields 1, 3, 4, 7, and 8 (V9 vs. V11, V14, V17, V15, and V15), which may have resulted in increased variability in CI values due to the lack of canopy closure. Direction-of-travel semivariance was greatest in Field 5 (1.0 at 75 m) and Field 6 (0.6 at 75 m). We attribute this outcome to the rolling terrain of the fields and the impact of this soil and landscape variation on stand and crop growth. Both fields contain multiple soil series and substantial variation in elevation (~8–10 m relief). These changes in relief have resulted in eroded hillslopes in each field, contributing to variability in topsoil quality and depth, ultimately contributing to spatial variability in N uptake and crop response to applied N across each field. High lateral and direction-of-travel variability in Field 5 may be due to its sandy texture being highly responsive to N fertilizer. On the basis of this analysis, the spatial structure of CI in the direction-of-travel in Fields 2, 5, and 6 was strong (significant rise of semivariogram beyond 22 m), which presented a situation suitable for variable-rate fertilizer management. Fields 1, 3, 4, 7, and 8 indicated that CI estimates varied from row to row more than within a given row, suggesting that variable-rate fertilization on these fields would not be advantageous.

MSE Comparison

While the analysis of spatial structure revealed general relationships among CI measurements, MSE was used to quantify the true loss of sensor information value when aggregating measurements across multiple rows and/or applying measurements obtained from one row to another. In all fields, there was an overall decrease in MSE with an increasing number of sensors (Fig. 3). This was due to the fact that multiple sensor measurements reduced the probability of incorrectly estimating the means, and the reduction was most significant with a lower number of sensors (MSE reduction was greater when using 2 sensors instead of 1 than when using 10 sensors instead of 9). However, with a relatively low number of sensors (less than 12), both empirical and analytical estimates of MSE were lower for single rate scenarios compared with the one-sensor-per-boom-section approach. This meant that, with high row-to-row variability of CI, it was better to calculate an average CI for the entire boom (24 rows) than to use each sensor to account for changing crop status in two rows or more.

The peaks measured with two to four sensors in the empirical data again suggested a systematic pattern in CI values between rows. This pattern was accentuated when sensors were sparsely placed along the boom. Smaller spikes could possibly be measured by selecting different rows (with smaller differences to the cross-row average). In each of the eight fields, there was a point at which splitting the boom into sections resulted in lower MSE than averaging sensors readings together across the entire boom. This occurred at 14 sensors for Fields 1 and 3, 8 sensors for Fields 2 and 5, 10 sensors for Fields 4 and 7, and 6 sensors for Fields 6 and 8. Therefore, a split boom assignment of CI and treating N deficiency symptoms accordingly may be reasonable for Fields 2, 5, and 6. The other fields required either treating each row independently or averaging CI measurements for the entire width of the study area. Averaging "one rate – theoretical" MSE estimates from all fields (Fig. 4) resulted in MSE values 26% lower for two sensors as compared with one, while adding an extra sensor further reduced MSE by 12%. Using additional sensors resulted in much smaller MSE reductions. A follow-up agroeconomic analysis is required to identify economic benefits that may be associated with different degrees of MSE reduction, and therefore, our conclusions were based only on rate of MSE reduction rather than the actual optimum calculated using the ratio of error reduction benefit versus sensor costs.

When considering all possible combinations of the number of sensors per section (1 through m) as shown in Fig. 5, we found that a single rate based on two to three sensors produced relatively low MSE values, compared with other scenarios with a reasonable total number of sensors. However, due to significant spatial structure in Fields 2, 5, and 6, it appears that a split boom approach with two to three sensors per section produced relatively low MSE estimates in these fields. The previously discussed eight-row systematic pattern suggests an opportunity for eight-row application equipment. Such an implement could be equipped with three sensors, providing a total of nine sensors per 24-row width of our study area. However, placing sensors in each row and providing split boom applications (row-by-row treatment) resulted in the lowest MSE values in each field.

Predictability of Systematic Patterns

On the basis of the systematic patterns detected in the lateral semivariograms, quantifying row-to-row bias to improve neighbor row measurement prediction seemed to be appropriate. Analysis of per-row CI averages for Fields 2 and 4 showed a linear relationship (R^2 = 0.32 and 0.19) between CI values and number of rows from the center of each eight-row section (Fig. 6B and 6D). The relationship for Fields 1 and 3 (R^2 = 0.50 and 0.42) was found to be nonlinear (Fig. 6A and 6C). A row-to-row systematic pattern in CI (R^2 = 0.40) was detected in Field 5 (Fig. 6E), while no relationship (R^2 < 0.01) between CI and row position was detected in Fields 6, 7, or 8 (Fig. 6F–6H). Table 3 shows CI adjustment values that can be applied to average row CI measurements based on the row position from the center of the eight-row pass within Fields 1 through 5. These values were obtained from a series of linear and nonlinear regression analyses between the relative position with respect to the center of eight-row application and CI. Once cross-row average CI is known, CI estimates for individual rows can be adjusted according to the number of rows from the center of an eight-row implement. This produced average row-to-row profiles shown in Fig. 7 and resulted in 20 to 67% MSE reduction when 24 sensors were used to predict a variable-rate based on a per-boom CI average (Table 3). The results suggested that row-to-row trends can be used to fine-tune sensor placement along the boom. When a sensor is assigned to a lower-than-average or higher-than-average row, an adjustment factor from Table 3 could be used to account for the sensor

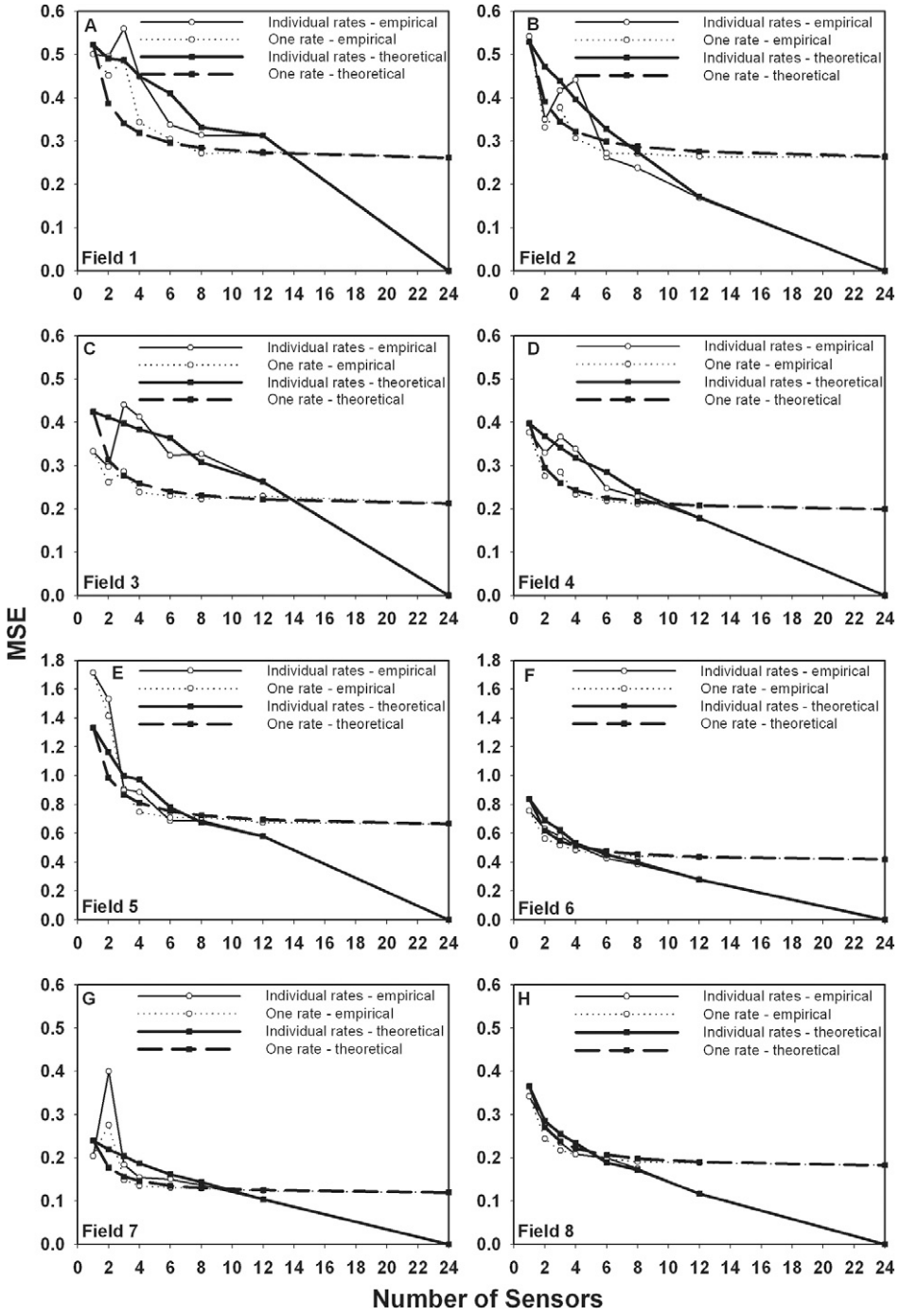

←Fig. 3. Theoretical and empirical mean square error (MSE) estimates when averaging CI values for the entire boom and assuming individual sensor measurements to represent entire boom sections in Fields 1 through 8 (A through H). Note different MSE scales for Fields 5 and 6.

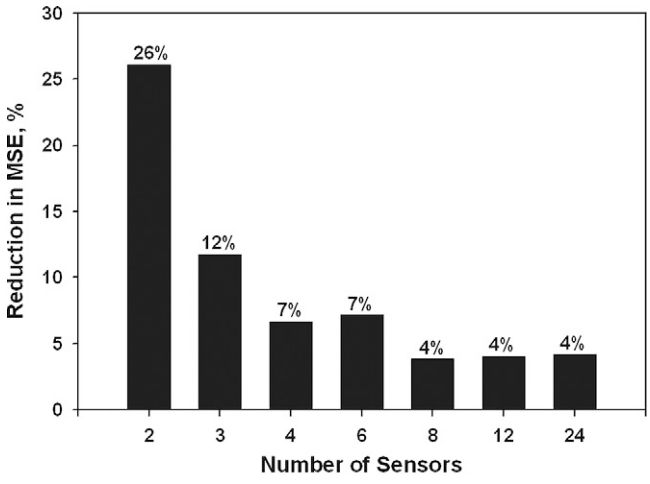

←Fig. 4. Percentage reduction in mean square error (MSE) versus increasing number of sensors (based on average across all fields of "one rate–theoretical" scenario in Fig. 2).

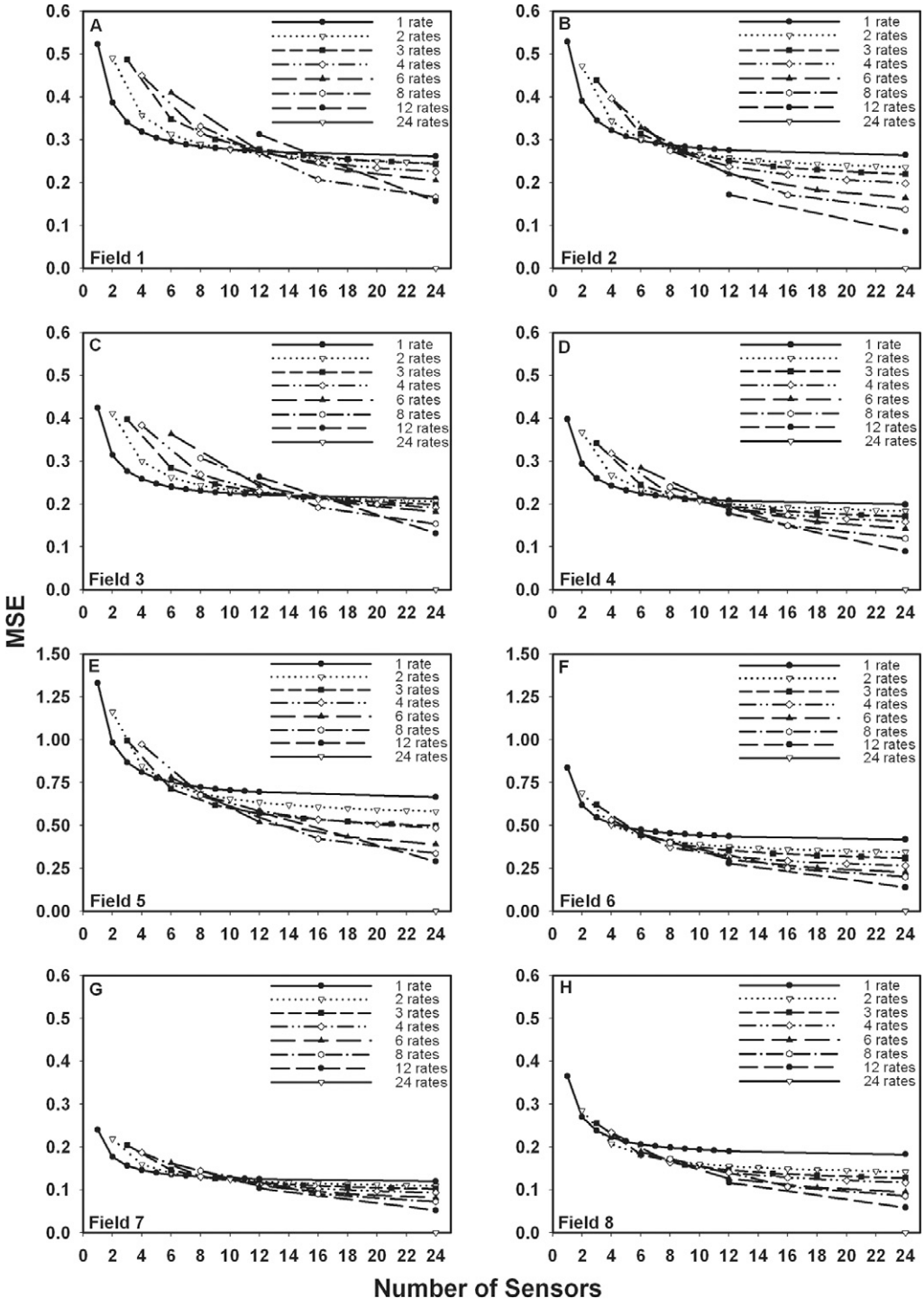

Fig. 5. Evaluation of mean square error (MSE) versus increasing number of sensors with split-boom N application scenarios in Fields 1 through 8 (A–H). Note different MSE scales for Fields 5 and 6.

Table 3. Chlorophyll Index (CI) adjustment values to account for row-to-row variability of average CI measurements based on the row position from the center of the planter for Fields 1–5.† MSE was reduced through variable rate application accounting for row-to-row CI variability (adjustment) compared with one variable rate applied across the entire boom (one rate).

Field ID	Number of rows from the center of planter				MSE		
	0	1	2	3	One rate	Adjustment	Reduction
							%
1	+0.25‡	–0.25	–0.25	+0.25	0.29	0.20	32
2	–0.23	–0.08	+0.08	+0.23	0.72	0.24	67
3	+0.11	+0.11	+0.11	–0.32	0.22	0.18	20
4	–0.11	–0.04	+0.04	+0.11	0.25	0.19	21
5	–0.28	+0.28	-0.28	+0.28	1.50	0.59	61

† Predictable row-to-row variability was not detected in Fields 6–8.

‡ Values indicate appropriate adjustment of per boom average measurement.

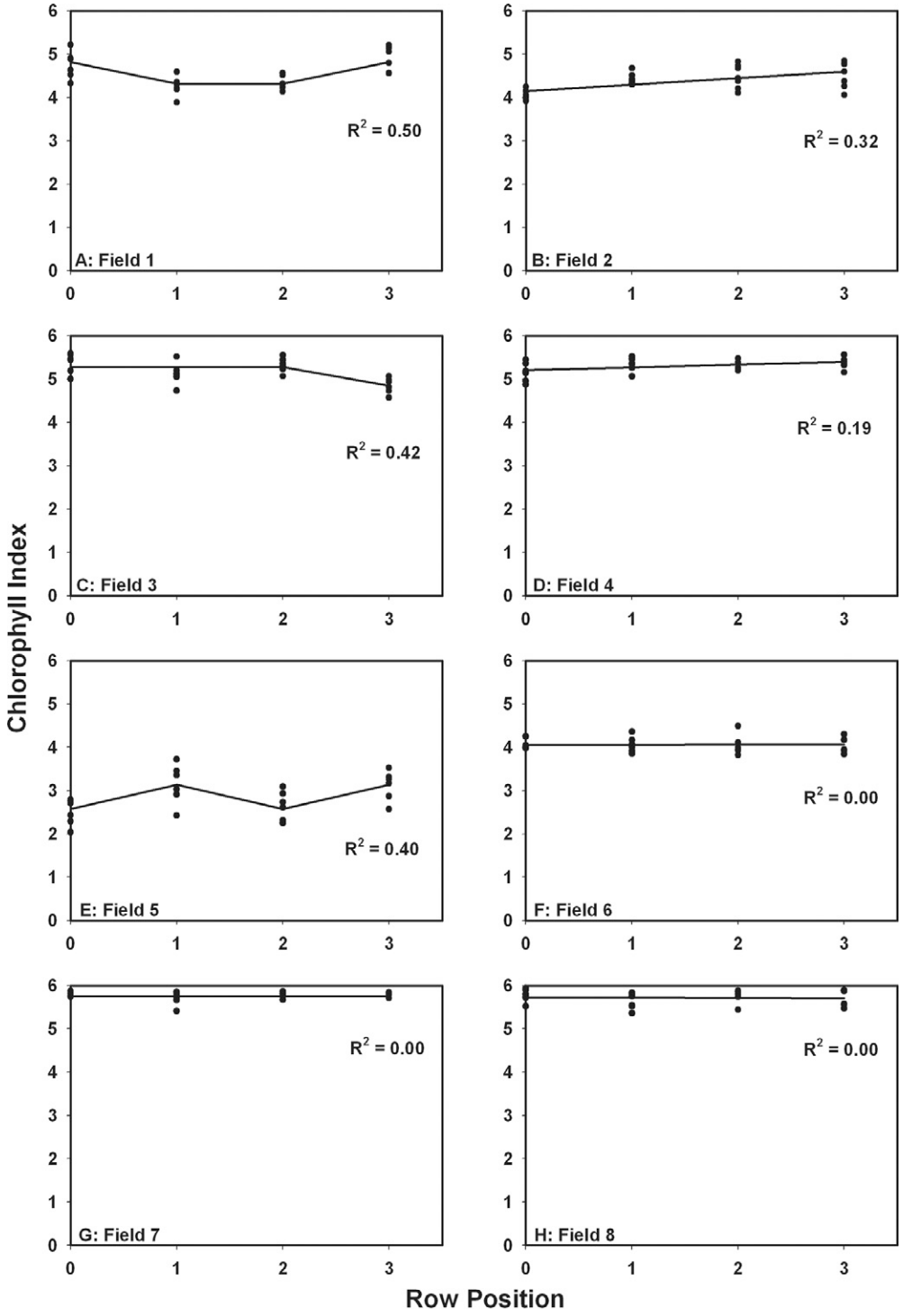

Fig. 6. Relationship between chlorophyll index and row position based on three, eight-row strips (0 = next to the center of eight rows, 3 = outside row of eight-row strip).

placement before averaging CI values from different rows. Sizing nozzles to account for systematic row-to-row variability is another feasible solution. Such strategies would require knowledge of row trends prior to in-season management. In the cases when significant lateral spatial structure exists, an interpolation technique can be used to predict CI values for a row without a sensor instead of simply assuming the closest measurement or average.

Based on the overall comparison of MSE estimates for different approaches to estimate CI values across the field (Fig. 8), it appears that fixed rate N-management (assumption of constant CI) resulted in high MSE in Fields 2, 5, and 6. Field 7, on the other hand, was the most uniform. Assigning a row-specific average CI slightly reduced MSE in all fields. Variable-rate application using a single estimate of CI (true mean) per 24 rows was found to be lower for Fields 2, 5, and 6, and somewhat lower for Fields 4, 7, and 8. These single-variable-rate scenarios require 24 sensors, which would be the most expensive option of all the scenarios considered. When using only three sensors to average one CI per entire 24-row section, MSE

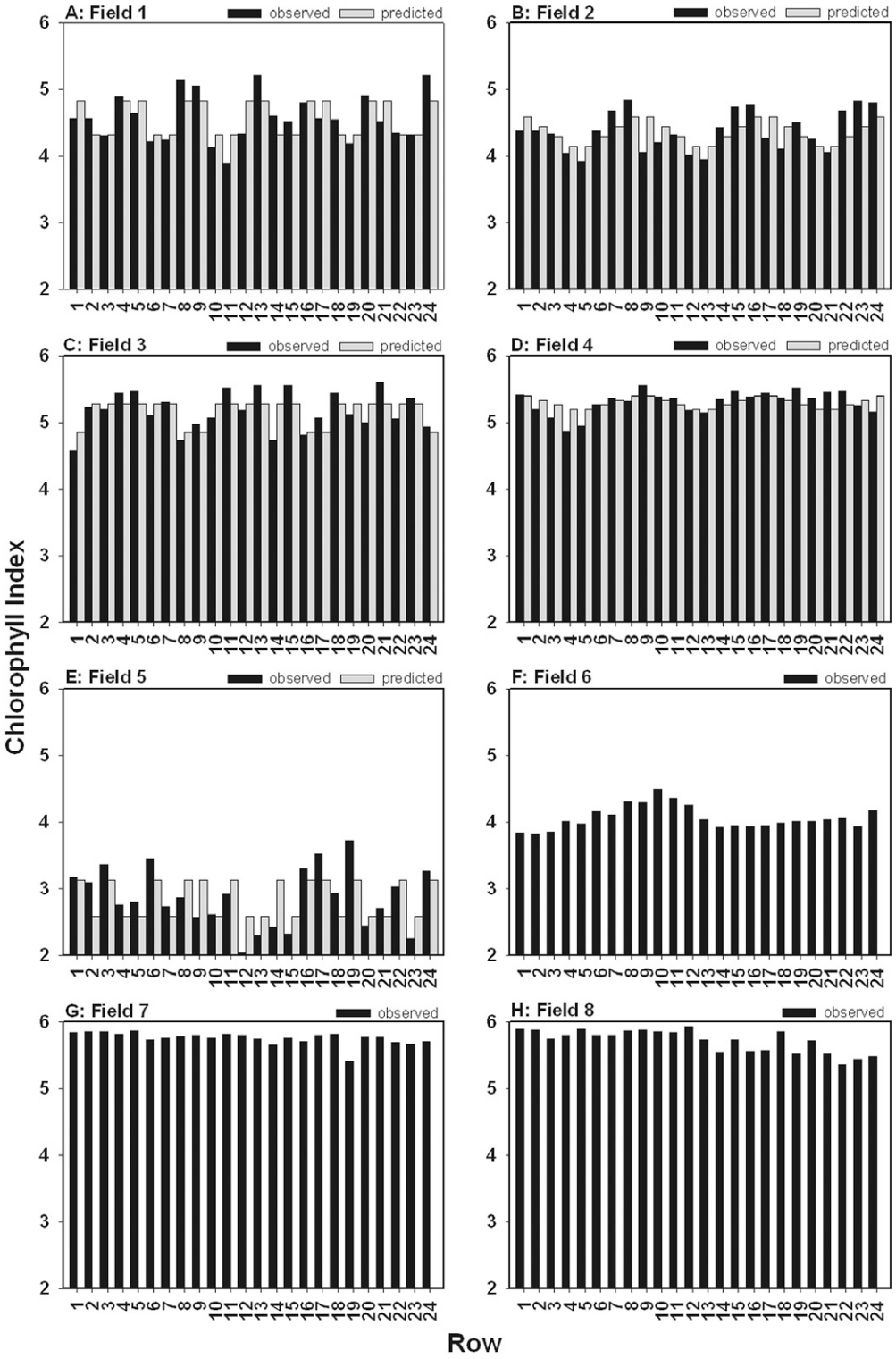

Fig. 7. Actual and modeled distributions of row-to-row mean variability of chlorophyll index (CI) measurements for Fields 1 through 5. The CI was not modeled for Fields 6, 7, or 8 because no significant relationship between CI and row position was detected.

values increased, and caused variable rate application for Fields 1, 3, and 4 to be nonefficient. Using an eight-row implement or applying systematic pattern recognition somewhat reduced MSE in each field, making it the same or below MSE estimates for the fixed rate scenarios. Only Fields 2, 5, and 6 indicated significant improvement of CI predictability when pursuing the variable-rate approach.

Ultimately, because treating each row of corn according to individual CI measurement is likely not feasible due to high sensor and equipment costs, average CI values can be applied using two to three sensors for each section, providing a single unbiased CI estimate. Identification of row-to-row trends can further improve predictability. However, variable-rate N management to account for changing CI measurements could

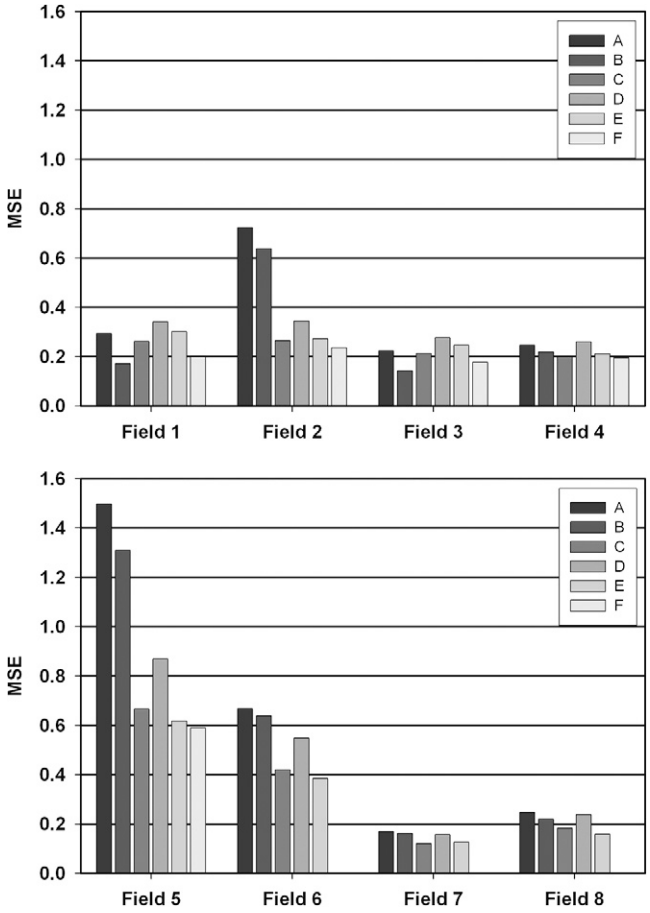

Fig. 8. Mean square error (MSE) of (A) single fixed N rate, (B) row-specific fixed N rate, (C) single variable rate (mean of 24 sensors), (D) single variable rate (3 sensor average), (E) 8-row variable rate (3 sensor average) for Fields 1 through 8, and (F) identification of row-to-row systematic pattern plus variable rate for Fields 1 through 5.

be efficient only if row-to-row variability of CI is smaller than variability down the row, as was found in Fields 2, 5, and 6.

CONCLUSIONS

In this study, the ability to minimize the number of canopy sensors used to measure chlorophyll index (CI) in corn was found to depend on the site. An average of two to three sensors should be an acceptable approach to obtain a single application rate for the entire boom, assuming the boom is not longer than the width of our study areas (22 m). Three of eight sites indicated a potential benefit of splitting the boom into three sections with two to three sensors per section. Relatively high row-to-row variability signified low predictability of CI based on sensor measurements obtained from a neighbor row. In fact, due to management-induced systematic patterns, we found CI measurements from rows equidistant from the center of an eight-row planter had more similarities than rows next to each other. The ability to model this variability provided some improvement over a single-rate approach. Relatively low CI variability in the direction of travel detected in five of the eight measured fields caused varying N rate, based on the averaged or modeled CI prediction from a few sensors, to be inappropriate. However, significant CI variability across Fields 2, 5, and 6 suggested potential benefit to site-specific N management practices based on active crop canopy reflectance sensors. It appears that in-season variable rate N management with the number of sensors substantially lower than the number of rows is suitable only when field variability of CI is greater than the variability from row-to-row. Splitting the 24-row boom into smaller sections can be advantageous only if significant spatial structure across the boom can be detected. However, even in such situations, any application rate should be based on the average of two to three sensors rather than a single sensor per individual rate. A one-sensor-per-rate scenario is the ultimate solution for fields with high row-to-row variability relative to the overall field variability when every row is sensed independently.

REFERENCES

Adamchuk, V.I., M.T. Morgan, and J.M. Lowenberg-Deboer. 2004. A model for agro-economic analysis of soil pH mapping. Prec. Agric. 5:111–129.

Cassman, K.G., A. Dobermann, and D.T. Walters. 2002. Agroecosystems, nitrogen-use efficiency, and nitrogen management. Ambio 31:132–140.

FAO. 2008. FAOSTAT. Available at http://faostat.fao.org/site/422/default.aspx [verified 21 Aug. 2008]. Food and Agriculture Organization of the United Nations, Rome.

Gitelson, A.A., Y. Gritz, and M.N. Merzlyak. 2003. Relationships between leaf chlorophyll content and spectral reflectance and algorithms for non-destructive chlorophyll assessment in higher plant leaves. J. Plant Physiol. 160:271–282.

Gitelson, A.A., Y.J. Kaufman, and M.N. Merzlyak. 1996. Use of a green channel in remote sensing of global vegetation from EOS-MODIS. Remote Sens. Environ. 58:289–298.

Gitelson, A.A., A. Vina, V. Ciganda, D.C. Rundquist, and T.J. Arkebauer. 2005. Remote estimation of canopy chlorophyll content in crops. Geophys. Res. Lett. 32:L08403, doi:10.1029/2005GL022688.

Pena-Yewtukhiw, G.J. Schwab, J.H. Grove, L.W. Murdock, and J.T. Johnson. 2008. Spatial analysis of early wheat canopy normalized difference vegetative index: Determining appropriate observation scale. Agron. J. 100:454–462.

Raun, W.R., and G.V. Johnson. 1999. Improving nitrogen use efficiency for cereal production. Agron. J. 91:357–363.

Raun, W.R., J.B. Solie, G.V. Johnson, M.L. Stone, R.W. Mullen, K.W. Freeman, W.E. Thomason, and E.V. Lukina. 2002. Improving nitrogen use efficiency in cereal grain production with optical sensing and variable rate application. Agron. J. 94:815–820.

Raun, W.R., J.B. Solie, M.L. Stone, K.L. Martin, K.W. Freeman, R.W. Mullen, H. Zhang, J.S. Schepers, and G.V. Johnson. 2005. Optical sensor-based algorithm for crop nitrogen fertilization. Commun. Soil Sci. Plant Anal. 36:2759–2781.

Scharf, P.C., J.P. Schmidt, N.R. Kitchen, K.A. Sudduth, S.Y. Hong, J.A. Lory, and J.G. Davis. 2002. Remote sensing for nitrogen management. J. Soil Water Conserv. 57:518–524.

Schepers, J.S., G.E. Varvel, and D.G. Watts. 1995. Nitrogen and water management strategies to reduce nitrate leaching under irrigated maize. J. Contam. Hydrol. 20:227–239.

Shanahan, J.F., N.R. Kitchen, W.R. Raun, and J.S. Schepers. 2008. Responsive in-season nitrogen management for cereals. Comput. Electron. Agric. 61:51–62.

Solari, F. 2006. Developing a crop based strategy for on-the-go nitrogen management in irrigated cornfields. Ph.D. diss. Univ. of Nebraska, Lincoln.

Solari, F., J. Shanahan, R. Ferguson, J. Schepers, and A. Gitelson. 2008. Active sensor reflectance measurements of corn nitrogen status and yield potential. Agron. J. 100:571–579.

Solie, J.B., W.R. Raun, and M.L. Stone. 1999. Submeter spatial variability of selected soil and Bermudagrass production variables. Soil Sci. Soc. Am. J. 63:1724–1733.

Solie, J.B., W.R. Raun, R.W. Whitney, M.L. Stone, and J.D. Ringer. 1996. Optical sensor based field element size and sensing strategy for nitrogen application. Trans. ASAE 39:1983–1992.

Varvel, G.E., J.S. Schepers, and D.D. Francis. 1997. Ability for in-season correction of nitrogen deficiency in corn using chlorophyll meters. Soil Sci. Soc. Am. J. 61:1233–1239.

Varvel, G.E., W.W. Wilhelm, J.F. Shanahan, and J.S. Schepers. 2007. An algorithm for corn nitrogen recommendations using a chlorophyll meter based sufficiency index. Agron. J. 99:701–709.